Journal of Achievements in Materials and Manufacturing Engineering
VOLUME 47
ISSUE 1
July
2011

Effects of deformation rates on mechanical properties of PP/SEBS blends

O. Balkan [a,*], H. Demirer [b], E. Sabri Kayalı [c]
[a] Department of Materials, Institute of Pure and Applied Sciences, Marmara University, Göztepe Campus, 34722, Kadıköy-İstanbul, Turkey
[b] Department of Materials, Technical Education Faculty, Marmara University, Göztepe Campus, 34722 Kadıköy-İstanbul, Turkey
[c] Department of Materials and Metallurgy, Chemistry-Metallurgy Faculty, İstanbul Technical University, Ayazağa Campus, 34469 Maslak-İstanbul, Turkey
* Corresponding author: E-mail address: obalkan@marmara.edu.tr

Received 10.05.2011; published in revised form 01.07.2011

Properties

ABSTRACT

Purpose: The goal of this study is to examine effects of tensile deformation rates ($\dot{\varepsilon}$) on tensile properties of polypropylene/poly(styrene-b-ethylene-co-butylene-b-styrene) copolymer (PP/SEBS) blends and to determine suitable $\dot{\varepsilon}$ for accurate and reliable evaluation of mechanical properties of the blends in accordance with the results of Izod impact tests.
Design/methodology/approach: PP/SEBS blends containing φ_e = 0, 2.5, 5 and 10 volume % of SEBS thermoplastic elastomer were compounded using a twin-screw extruder, and then moulded with an injection moulding machine. Morphology of PP/SEBS blends were analysed by scanning electron microscopy (SEM). Mechanical properties of the blends were investigated tensile and Izod impact tests. Tensile deformation rates $\dot{\varepsilon}_1$= 1.67 ms^{-1} and $\dot{\varepsilon}_2$ = 16.67 ms^{-1} were used to determine ultimate tensile properties.
Findings: Morphological analyses revealed that SEBS elastomer particles were well-dispersed throughout PP matrix in irregular forms with a narrow size distribution and evidenced a two-phase system formation. At low deformation rate ($\dot{\varepsilon}_1$), PP and PP/SEBS blends did not fail during tensile tests despite maximum tensile deformation, ε_{max} = 600%; therefore, tensile toughness (U_T), stress and strain values at break point (σ_b and ε_b) of the blends were not determined. However, at high deformation rate ($\dot{\varepsilon}_2$), all specimens tested in this study failed; a slight decrease in σ_b of the blends with SEBS elastomer was associated with a significant increase in ε_b and U_T. Strain-rate-sensitivity of PP/SEBS blends was promoted with SEBS elastomer.
Research limitations/implications: Mechanical properties determined through high-velocity tests are beyond the scope of this study.
Practical implications: $\dot{\varepsilon}$ of tensile testing machines is readily adjustable, while ε_{max} of tensile testing machines is limited. Consequently, in order to evaluate reliably mechanical properties of ductile materials like PP/SEBS blends, $\dot{\varepsilon}$ must be so high that ductile materials can fail during tensile tests.
Originality/value: Tensile testing at high strain rate $\dot{\varepsilon}_2$ was concluded to be more suitable for evaluation of mechanical properties of PP/SEBS blends than that of at low strain rate $\dot{\varepsilon}_1$.
Keywords: Tensile deformation rate; Polypropylene blends; SEBS thermoplastic elastomer

Reference to this paper should be given in the following way:
O. Balkan, H. Demirer, E. Sabri Kayalı, Effects of deformation rates on mechanical properties of PP/SEBS blends, Journal of Achievements in Materials and Manufacturing Engineering 47/1 (2011) 26-33.

1. Introduction

Polypropylene (PP) has been widely used in many scientific, industrial, and domestic appliances because of its well-known versatile properties and relatively low cost. Moreover, its outstanding properties can be modified easily by adding various polymers and rigid fillers using a suitable melt-mixing method. However, PP is sensitive to a notch and suffers from brittle fracture problems especially at low temperatures ($T<T_g$), although it is soft enough to scratch by means of finger nail at room temperature. Thus, mechanical properties of PP have been modified commonly by adding elastomers like SEBS as a toughening agent via a suitable melt-mixing method.

Recently, poly(styrene-*b*-ethylene-*co*-butylene-*b*-styrene) copolymer (SEBS) has been increasingly used to improve toughness of PP systems [1-9]. Physical interaction can take place between PP and SEBS because of similar chemical structure of PP to ethylene-*co*-butylene (EB) midblock of SEBS although PP and styrenic block of SEBS are incompatible. Comparing conventional elastomers, apparent increase in ductility of PP with addition of SEBS at low contents was reported to be associated with acceptable decrease in stiffness, resulting in a better mechanical performance [2,9]. However, studies dealing with strain rate effects on mechanical and morphological properties of PP/SEBS blends are scarce, while such studies on PP [10] toughened with ethylene-propylene-rubber (EPR) [11,12], ethylene-propylene-diene monomer (EPDM) [13,14] and acrylnitril-butadiene-rubber (NBR) [15] were well-documented in literature.

Mechanical properties of a material can be evaluated more accurately if suitable mechanical tests are performed according to properties of the material. In other words, to evaluate mechanical properties of a material more reliably, suitable mechanical tests must be adjusted according to properties of the material. Goal of this communication is to demonstrate effects of tensile deformation rates ($\dot{\varepsilon}$) on tensile properties of PP/SEBS blends and to determine suitable $\dot{\varepsilon}$ for accurate and reliable evaluation of mechanical properties of the blends in accordance with the results of Izod impact tests.

2. Experimental

2.1. Materials and preparation of specimens

Isotactic-polypropylene homopolymer (PP; Petoplen™ MH418) supplied by Petkim Petrochemical Holding Inc. was used as a matrix material. It has a melt flow rate (MFR) of 4-6 dg min^{-1} (g/10 min) at 230°C (2160 g) and a density of ρ = 0.886 g cm^{-3}. Poly(styrene-*b*-ethylene-*co*-butylene-*b*-styrene) block copolymer (SEBS; Kraton™ G-1652) supplied kindly by Kraton Polymers LLC was used as thermoplastic elastomer. SEBS having a density of ρ = 0.91 g cm^{-3} is linear triblock copolymers with ~30% of styrene.

PP was compounded with SEBS elastomer using an intermeshing co-rotating twin-screw extruder (Thermo Prism, Haake, a screw diameter of 16 mm, an L/D ratio of 25) at a screw speed of 100 rpm. Barrel temperature profile was set at 150, 230, 230, 230, and 230°C from feed zone to die. PP/SEBS binary blends contained φ_e = 0, 2.5, 5, and 10 volume % of SEBS elastomer. Strands obtained from the extruder were quenched immediately in water and then pelletized. The pellets were dried in an oven at 80°C for 48 h, and then molded under identical conditions using a conventional injection molding machine where mounted with a standard mold as shown in Fig. 1. Barrel temperature of the injection molding machine was set at 230°C, and mold temperature was set at 40°C.

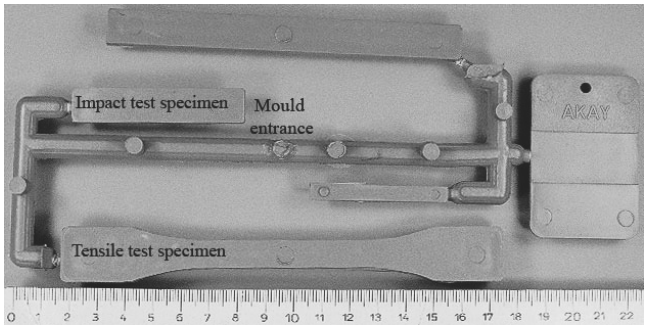

Fig. 1. A set of the injection molding specimens

2.2. Testing

In order to check the ratios of SEBS experimentally in the blends, density of the specimens was measured according to the standard EN (European Norms) 1183. Rheological properties of the blends were determined by means of Melt Flow Rate (MFR) using a MFR machine of Zwick 4100 model following the standard EN 1133. Composition and MFR results of the blends are tabulated in Table 1.

Longitudinal tensile properties of the specimens that were injection molded in a dumbbell-shape (type 1) with a thickness of 4 mm were measured using a Zwick Z010 model tensile testing machine at room temperature according to the standards EN 527-1 and -2. For *E*-modulus (*E*) determination in an extension range ε_E = 0.05-0.25%, tensile testing machine was set at a deformation rate $\dot{\varepsilon}_0$ = 0.33 ms^{-1} (cross-head displacement speed of V_0 = 1 mm min^{-1}; gauge length of L_0 = 50 mm; $\dot{\varepsilon} = V/L_0$). Tensile deformation rates of $\dot{\varepsilon}_1$ = 1.67 ms^{-1} and $\dot{\varepsilon}_2$ = 16.67 ms^{-1} (respective cross-head displacement speeds V_1 = 5 mm min^{-1} and V_2 = 50 mm min^{-1}) were used to determine ultimate tensile properties using an extensometer throughout the entire test course (ε_{max} = 600%).

Izod impact tests were carried out using a Zwick model impact testing machine with a pendulum of 5.5 J on the injection molded rectangular specimens of 12.5 × 3.2 × 62 mm^3 at room and liquid nitrogen temperatures following the standard EN 180. The notches were opened in perpendicular to the melt flow direction (MFD) with a Nothchvis-Ceast model V-notched cutter.

Table 1.
Composition and MFR results of PP/SEBS blends

Blends (φ_e)	Volume ratio φ (vol/vol)	Weight ratio W (wt/wt)	Density ρ (g cm^{-3})	Experimental φ (vol/vol)	MFR (dg min^{-1})
0.0	100.00 / **00.00**	100.00 / 00.00	0.881 *(0.2)*	100.00 / 0.00	5.23 *(053.9)*
2.5	097.50 / **02.50**	097.42 / 02.58	0.882 *(0.2)*	097.55 / 2.45	5.17 *(142.7)*
5.0	095.00 / **05.00**	094.85 / 05.15	0.883 *(0.6)*	095.47 / 4.53	5.05 *(071.0)*
10.0	090.00 / **10.00**	089.71 / 10.29	0.884 *(0.2)*	090.57 / 9.43	4.80 *(148.2)*

Standard deviations (S) × 10^3 are shown in parentheses (italic form)

For SEM analyses, a selective etching procedure was performed to reveal elastomeric phase structure of the blends. The fresh cryo-fractured specimens were immersed in a thermostated ultrasonic bath filled with xylene at room temperature for 20 min to dissolve elastomeric phases and then dried in a vacuum oven at 80°C for 4 h. Fresh cryo-fracture surfaces of the specimens were coated with gold and then analyzed with a JEOL JSM-5910LV model SEM at an acceleration voltage of 10 kV, and typical SEM micrographs were taken.

3. Results and discussion

3.1. SEM analyses

Any contrast between SEBS and PP phases was not detected on non-etched fracture surfaces of PP/SEBS blends, inferring high compatibility between SEBS and PP. However, after etching procedure, small dark holes were left on the surfaces of the blends as shown in Fig. 2. The holes indicating SEBS particles were in irregular forms, well-dispersed throughout PP matrix and evidenced a two-phase system formation. Affinity of polyolefinic EB midblock of SEBS with PP matrix could be responsible for the irregular shape of the holes [3].

Morphology of a polymer system is a result of a frozen dynamic equilibrium among factors such as shear stress, interfacial tension, compatibility, viscosity ratio, and content of components during melt mixing [16]. Mean size of the holes was measured to be nearly 0.3 μm with a narrow size distribution. Whereas their size did not varied significantly, the number of the holes increased with increasing SEBS content. The narrow range of elastomer contents, high compatibility of the blends, high shear forces during melt-mixing in the twin-screw extruder, and further mixing and quick solidification during the subsequent injection molding probably caused the elastomer particle size not to increase with increasing elastomer content.

3.2. Tensile properties

Variations in stress (σ) of PP/SEBS blends with strain (ε) at strain rates of $\dot{\varepsilon}_1$ = 1.67 ms^{-1} and $\dot{\varepsilon}_2$ = 16.67 ms^{-1} are shown in Fig. 3a and b. At both deformation rates ($\dot{\varepsilon}_1$ and $\dot{\varepsilon}_2$), tensile behavior of PP/SEBS blends was characterized by a typical yield peak that was followed by stress drop due to initiation of necking phenomenon and probably to stress softening. Because each of the amorphous and crystalline phases in PP/SEBS yields at different strain ratios in microscopic scale, the yield peaks of the bends are not sharp. At the maximum of the yield peak, necking begins where crazing/shear band density is a maximum.

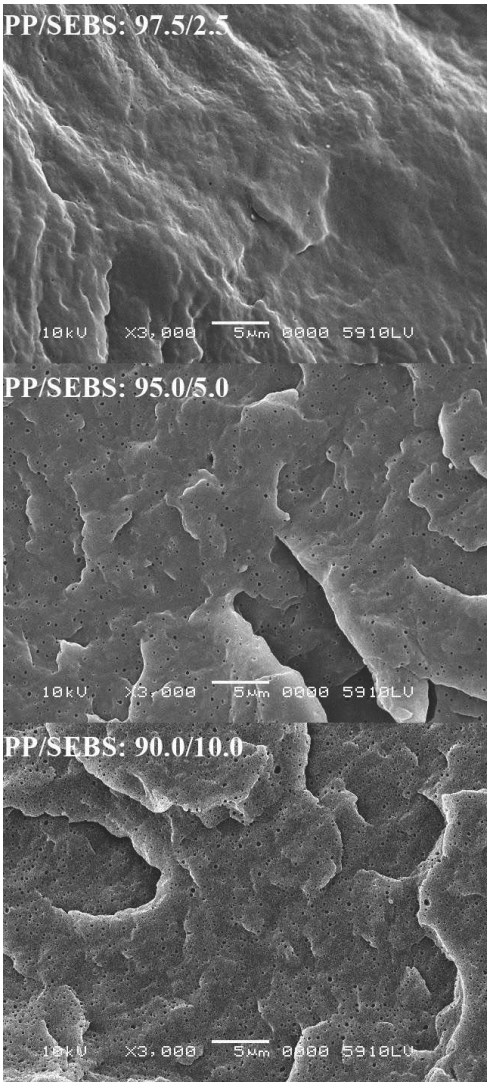

Fig. 2. SEM micrographs of etched PP/SEBS blends. From above downwards, φ_e = 2.5, 5 and 10

The yield peak became lower and broader gradually with increasing SEBS. Necking started later with SEBS, due probably to the fact that SEBS elastomer exhibited no yield peak and no necking consistently. Extension of SEBS particles showing no yield behavior may overlap the yield behavior of PP, thus the yield peak of PP was widened and suppressed with SEBS [2]. After stress drop due to necking, PP/SEBS blends exhibited a slight increase in stress because the neck propagated along the gauge length up and down, resulting in orientation of PP chains and an increase in crystallinity of PP (strain hardening).

As shown in Figures 3a and 4a, at low deformation rate ($\dot{\varepsilon}_1$), PP and PP/SEBS blends did not fail during tensile tests despite ε_{max} = 600%. However, at high deformation rate ($\dot{\varepsilon}_2$), all specimens tested in this study failed as shown in Figures 3b and 4b. For φ_e = 0, 2.5 and 5 vol % SEBS, failure started at center of the deformed region and proceeded fast normal to the applied stress direction with rough fracture surfaces (Fig. 4b). For φ_e = 10 vol % SEBS, failure occurred suddenly and fibrously due to distinct orientation.

Data obtained from the stress-strain curves of PP/SEBS blends are listed in Table 2. *E*-modulus is an important parameter characterizing resistance to deformation (*i.e.*, stiffness) of materials. As expected, *E*-modulus of PP/SEBS blends decreased with SEBS due to the substitution of PP matrix by soft SEBS elastomer. Yield stress σ_y can be regarded as an upper allowable stress limit without considerable plastic deformation. At both deformation rates ($\dot{\varepsilon}_1$ and $\dot{\varepsilon}_2$), σ_y decreased with SEBS, suggesting a decrease in load-bearing-cross-section of PP with SEBS due to low strength of SEBS elastomer. Yield strain ε_y of PP increased linearly with SEBS at both deformation rates ($\dot{\varepsilon}_1$ and $\dot{\varepsilon}_2$). The substitution of PP matrix by ductile SEBS caused elongation of PP to increase.

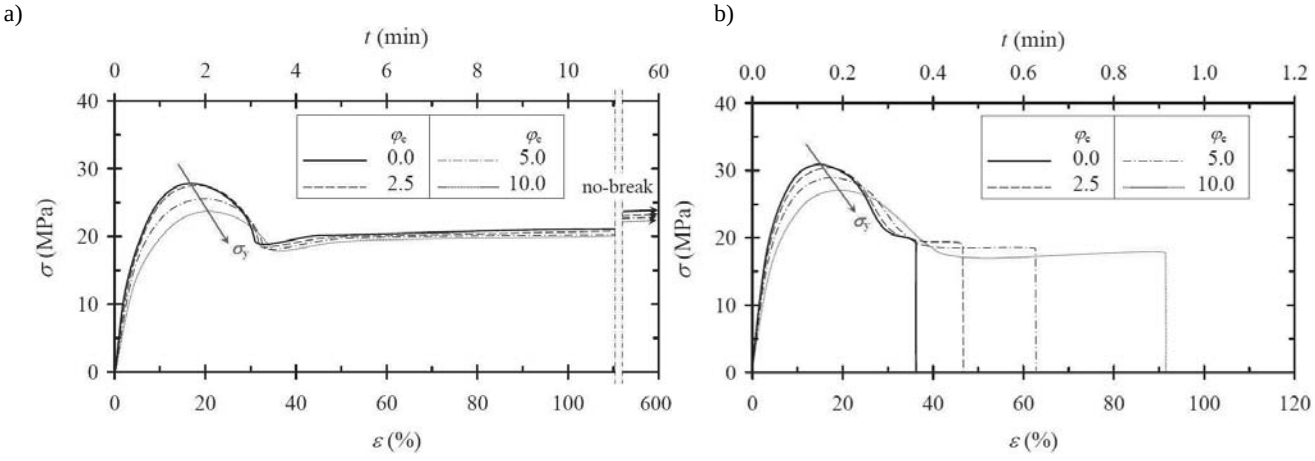

Fig. 3. Stress-strain (σ-ε) curves of PP/SEBS blends. (a) $\dot{\varepsilon}_1$ = 1.67 ms^{-1}, (b) $\dot{\varepsilon}_2$ = 16.67 ms^{-1}

Table 2.
Tensile properties of PP/SEBS blends

Blends (φ_e)	*E* (GPa)	σ_y (MPa)	ε_y (%)	U_R[a] (J m^{-3} 10^8)	σ_b (MPa)	ε_b (%)	U_T[a] (J m^{-3} 10^8)
$\dot{\varepsilon}_0$ = 0.33 ms^{-1} for *E*-modulus; $\dot{\varepsilon}_1$ = 1.67 ms^{-1} for ultimate properties:							
0.0	1.02 *(13)*	28.02 *(179)*	16.23 *(293)*	340.38	no break	>600	-
2.5	0.92 *(14)*	27.62 *(149)*	17.67 *(500)*	378.02	no break	>600	-
5.0	0.81 *(17)*	25.70 *(221)*	19.17 *(115)*	380.33	no break	>600	-
10.0	0.70 *(23)*	23.88 *(114)*	21.07 *(443)*	379.58	no break	>600	-
$\dot{\varepsilon}_0$ = 0.33 ms^{-1} for *E*-modulus; $\dot{\varepsilon}_2$ = 16.67 ms^{-1} for ultimate properties:							
0.0	1.07 (2)	31.07 (050)	14.71 (392)	284.28	19.42 (706)	35.94 (862)	884.32
2.5	0.96 *(1)*	30.64 *(182)*	16.07 *(109)*	319.08	18.95 *(708)*	46.72 *(976)*	1069.12
5.0	0.85 *(1)*	29.03 *(195)*	17.12 *(082)*	310.56	18.36 *(712)*	62.84 *(953)*	1340.72
10.0	0.73 *(2)*	27.08 *(358)*	18.72 *(497)*	289.03	17.82 *(694)*	91.28 *(909)*	1783.44

[a] Unit $U_{R,T}$ = (N m^{-2} 10^6) × (m m^{-1} 10^2) = J m^{-3} × 10^8. $S \times 10^3$ are shown in parentheses (italic form)

a)

b)

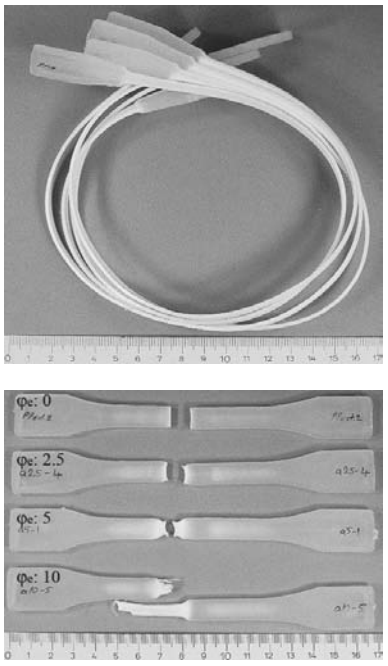

Fig. 4. Tensile tested specimens. (a) PP, $\dot{\varepsilon}_1$ = 1.67 ms^{-1}. (b) PP/SEBS blends (from above downwards, φ_e = 0, 2.5, 5 and 10), $\dot{\varepsilon}_2$ = 16.67 ms^{-1}

With increasing strain rates from $\dot{\varepsilon}_1$ to $\dot{\varepsilon}_2$, an increase in σ_y of the blends was associated with a decrease in ε_y. That is, increasing strain rate resulted in a more brittle response due to shorting time for molecular relaxation. At high strain rates and low temperatures, neither crystallization nor deformation mechanisms dissipating deformation energy are expected to have sufficient time to develop. Effects of strain rate and temperature on yield stress can be described by Eyring with respect to stress-activated flow process [17]. For the sake of simplicity, effects of strain rate on σ_y and ε_y (*i.e.*, strain-rate-sensitivity) can be expressed readily by parameters *m* and *n* as given

$$\sigma_2 = \sigma_1\left(1 + m\ln\frac{\dot{\varepsilon}_2}{\dot{\varepsilon}_1}\right), \tag{1}$$

$$\varepsilon_2 = \varepsilon_1\left(1 + n\ln\frac{\dot{\varepsilon}_2}{\dot{\varepsilon}_1}\right), \tag{2}$$

where σ_1 and σ_2 are yield stress, ε_1 and ε_2 are yield strain at $\dot{\varepsilon}_1$ and $\dot{\varepsilon}_2$; *m* and *n* are strain-rate-sensitivity-exponents, respectively, [18,19]. *Eqs. 1* and *2* mean that strain-rate-sensitivity increases with increasing *m* and decreasing *n*, due to an increase in yield stress and a decrease in yield strain with increasing strain rate. As shown in Fig. 5, main strain-rate-sensitivity of PP/SEBS blends was promoted with SEBS elastomer.

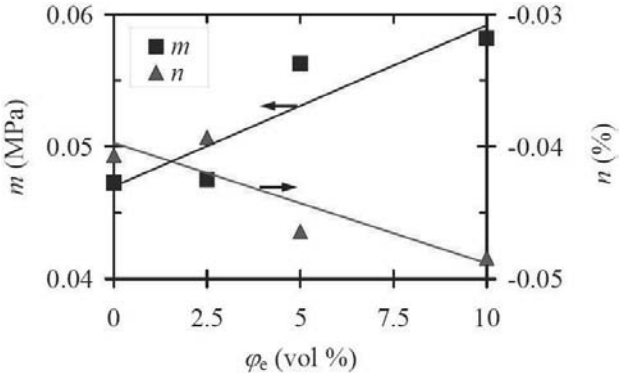

Fig. 5. Variations in strain-rate-sensitivity-exponents *m* and *n* with SEBS elastomer content (φ_e)

At low deformation rate ($\dot{\varepsilon}_1$), stress and strain values at break point (σ_b and ε_b) of the blends were not determined because they did not fail despite ε_{max} = 600%. At high deformation rate ($\dot{\varepsilon}_2$), a slight decrease in break stress (σ_b) of the blends with SEBS was associated with a significant increase in break strain (ε_b).

Energy absorption per unit volume of a material up to rupture (tensile toughness, U_T) is obtained from area underneath stress-strain curves. Besides, energy that is absorbed elastically per unit volume of a material (tensile elasticity, resilience, U_R) is also obtained from area underneath stress-strain curve in a strain range of 0-ε_y. U_R and U_T values of the blends are listed in Table 2. At $\dot{\varepsilon}_1$, a significant increase in U_R of PP with 2.5 vol % of SEBS was followed by a slight increase with 5 vol % of SEBS, where U_R of PP/SEBS is a maximum. At $\dot{\varepsilon}_1$, U_T of the blends was not determined because they did not fail despite ε_{max} = 600%. At $\dot{\varepsilon}_2$, U_R of PP reached a maximum only with the small content of SEBS. At $\dot{\varepsilon}_2$, U_T of PP increased linearly with SEBS. An increase in U_T with SEBS suggested that a part of deformation energy may be absorbed by elastomer particles undergoing sufficient elongation before fracture.

3.3. Izod impact properties

Unlike the notched specimens of PP/SEBS blends, the unnotched specimens of the blends did not fail during Izod impact testing (Table 3). This suggested that excessive energy was needed to initiate cracks in the unnotched specimens because the absence of a notch drastically increases the extent of plastic yielding prior to impact fracture. However, in the case of the notched specimens, notch tip acted as a site of stress concentration from which crack initiation developed much readily. Consequently, a large portion of impact energy was absorbed during crack initiation stage, and relatively very little portion of impact energy was consumed once a crack was propagating. Gupta and Purwar [4] found a decrease in notch-sensitivity of PP with SEBS due to an increase in ductility.

Table 3.
Izod impact test results of PP/SEBS blends

Blends	At room temperature		At liquid nitrogen temperature
	Unnotched (kJ m^{-2})	Notched (kJ m^{-2})	Notched (kJ m^{-2})
0.0	no break	3.50 *(283)*	4.25 *(300)*
2.5	no break	4.73 *(544)*	4.10 *(200)*
5.0	no break	5.50 *(294)*	3.93 *(222)*
10.0	no break	7.15 *(191)*	3.83 *(222)*

$S \times 10^3$ are shown in parentheses (italic form)

For elastomer-toughened polymers, it was proposed such energy dissipating deformation mechanisms as fracture of rubber particles after cavitation, debonding of rubber particles, shear band/craze interaction, transparticle fracture, crack deflection by rubber particles, diffuse shear yielding, plastic zone at crack tip, crazing, voided or cavitated particles, debonding of rubber particles, tearing of rubber particles, stretching, shear band formation near rubber particles,…*etc*. [20]. Materials in front of a notch tip can be subjected to plane-stress and plane-strain during applied impact loading (Fig. 6), and a large plastic zone ahead of the notch tip leads to a high toughness. At both sides of a notch, the response is plane-stress deformation at constant volume, involving a contraction in *z*-direction (like necking in tensile deformation). At the midpoint of the notch, stresses are triaxial. The reason for the state of triaxial tension is that the material in the tip of the notch is trying to contract in *z*-direction to maintain constant volume, but is unable to do so because it is constrained by the surrounding material. Transition from plane-strain to plane-stress is readily with elastomer due to an increase in shear yielding. At high temperatures, brittle-*to*-tough transition in fracture depends critically on strain rate. Gensler *et al.* [11] observed a decrease in size of yield zone ahead of crack tip with increasing test speed, suggesting a transition from plane-stress to plane-strain conditions.

In the applied stress direction σ, maximum stress concentration σ_{max} at the root of a notch is given by

$$\sigma_{max} = \sigma\left(1 + 2\sqrt{a/r_0}\right), \quad (3)$$

where a is notch depth, r_0 is radius of notch tip [21]. It is clear from *Eq. 3* that

$$\lim_{r_0 \to \infty} \sigma_{max} = \sigma$$

(*i.e.*, unnotched specimen);

$$\lim_{r_0 \to 0} \sigma_{max} = \infty$$

(*i.e.*, ideal sharp notch).

Using *Eq. 3*, in this study, $\sigma_{max} = 7.07\sigma$ can be calculated (a = 2.5 mm; r_0 = 0.25 mm). Effects of notch radius r_0 on fracture resistance are more striking in ductile materials than brittle materials. Most ductile materials like PP are notch-sensitive [21]. Impact energy falls rapidly with decreasing notch radius because the presence of a sharp notch drastically reduces extend of plastic yielding.

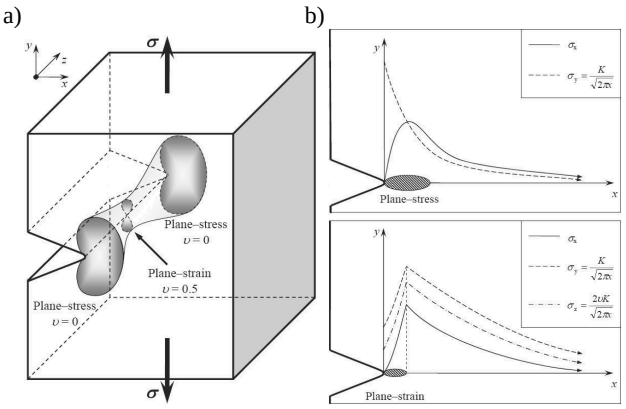

Fig. 6. (a) Yield zone and (b) stress distributions ahead of a notch (schematic); υ, Poisson ratio; K, stress-intensity factor

Comparing the tensile tests, strain rates in front of the notch tip are much higher, and plastic deformation (volume-related energy) is more limited due to much higher strain rates [22]. Crack propagates much faster through whole cross section of specimens with less plastic deformation during impact loading. Using equations of kinetic and potential energies, pendulum velocity V_{Impact} of the standard Izod test is calculated to be 3.46 ms^{-1}. According to Fig. 7, notch opening speed (V_{Notch}) can be expressed as

$$\tan\theta = \frac{V_{Impact}}{h} = \frac{V_{Notch}}{(w-a)/2} \quad (4)$$

where θ is deformation angle. In *Eq. 4*, (*w-a*)/2 was used instead of (*w-a*) because stress is assumed to be zero at nearly (*w-a*)/2. From *Eq. 4*, V_{Notch} was calculated to be 0.79 m s^{-1}. Assuming L_0 = 0.50 mm ($L_0 = 2r_0$), deformation rate at notch tip (*i.e.*, notch opening rate $\dot{\varepsilon}_{Notch} = V_{Notch}/L_0$) was calculated readily to be 1572.73 s^{-1} ≅ 1.57 ks^{-1}. Comparing the tensile deformation rates ($\dot{\varepsilon}_1$ = 1.67 ms^{-1}; $\dot{\varepsilon}_2$ = 16.67 ms^{-1}) used in this study, impact deformation rate ($\dot{\varepsilon}_{Notch}$ = 1.57 ks^{-1}) at the notch tip was calculated to be so much higher ($\dot{\varepsilon}_{Notch} \cong \dot{\varepsilon}_1 \times 10^6$ and $\dot{\varepsilon}_2 \times 10^5$).

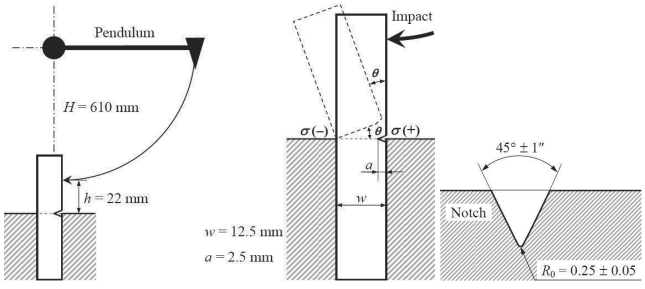

Fig. 7. Geometries and dimensions in Izod impact test

In accordance, Tjong *et al.* [23] found that volume-related plastic energy of PP based blends and composites was lower when impact tests were performed using a higher speed. Tam *et al.* [24] observed cavitation at EPR particles in slow crack propagation region of PP/EPR fracture surface, but it was absent in fast crack propagation region. In the present study, as shown in Fig. 8, any evidence of stress-whitening (multiple crazing) that is an energy-absorbing yield process was not observed at the fracture surfaces of PP/SEBS blends due probably to high speed of crack propagation. However, as given in Table 3, notched impact strength of PP at room temperature increased linearly with SEBS. *This suggested that some deformation mechanisms dissipating impact energy proceeded during impact loading despite fast crack propagation*. An increase in impact strength of PP with SEBS [4,6-9] was reported previously. Gensler *et al.* [11] reported that PP displayed a ductile-*to*-brittle transition as test speed was increased, which was associated with a transition from shear deformation to crazing. However, adding EPR to PP, deformation was characterized by stable crack propagation.

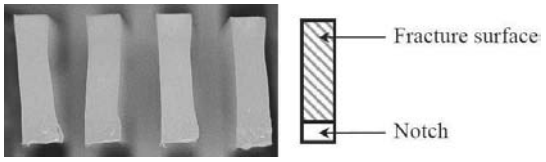

Fig. 8. Optical image showing fracture surfaces of PP/SEBS blends tested at room temperature. From left to right, φ_e = 0, 2.5, 5 and 10. Image contrast was increased slightly to clarify possible stress-whitening zones

It was found a good correlation of tensile toughness U_T and break strain ε_b at $\dot{\varepsilon}_2$ with notched impact strength *NIS*, as shown in Fig. 9. Because U_T and *NIS* both indicate energy absorbing by materials, a correlation of *NIS* with U_T seems to be more suitable and meaningful than with ε_b, although ε_b indicates ductility. At liquid nitrogen temperature, impact strength of the blends decreased with SEBS, indicating that SEBS elastomer did not act as toughening agent under T_g of SEBS ($T < T_g$; T_g of SEBS is nearly -49°C [6]).

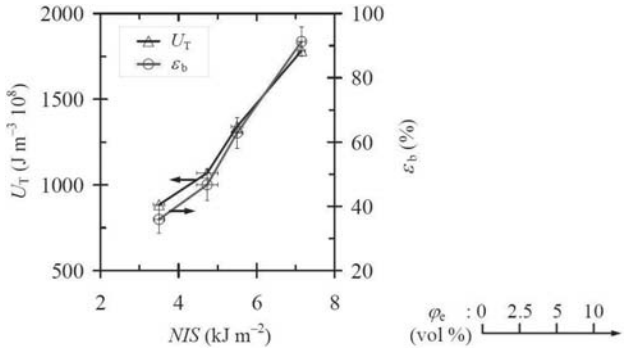

Fig. 9. Correlations of U_T and ε_b with *NIS* at room temperature. Error bars show *S* for *NIS* and *S* × 10 for ε_b

4. Conclusions

Toughness of PP increased with SEBS elastomer at the expense of stiffness and tensile strength. Tensile tests performed at two strain rates ($\dot{\varepsilon}_1$ and $\dot{\varepsilon}_2$) exhibited an increase in strain-rate-sensitivity of PP/SEBS blends with SEBS elastomer. At low strain rate $\dot{\varepsilon}_1$, despite ε_{max} = 600%, the blends did not fail during tensile test, so mechanical properties of the blends at break point were not determined. In other words, tensile tests of the blends were not able to be completed at low strain rate $\dot{\varepsilon}_1$. However, at high strain rate $\dot{\varepsilon}_2$, they failed, so their mechanical properties at break point were able to be evaluated. In accordance with the result of tensile toughness U_T obtained at $\dot{\varepsilon}_2$, notched impact strength *NIS* of PP/SEBS increased with increasing SEBS content. Consequently, tensile testing at high strain rate $\dot{\varepsilon}_2$ seemed to be more suitable for evaluation of mechanical properties of PP/SEBS blends than that of at low strain rate $\dot{\varepsilon}_1$. It was found that strain rate ($\dot{\varepsilon}$) must be so high that ductile materials like PP/SEBS blends can fail during tensile tests in order to evaluate reliably mechanical properties.

Acknowledgements

The authors would like to thank Prof. Dr. Ülkü Yılmazer, Güralp Özkoç, Özcan Köysüren, Sertan Yeşil and Mert Kılınç (METU) for their kind help during extrusion. Thanks also go to Sinan Kara from Kraton Polymers LLC for SEBS elastomer and Burak Erenoğlu from Akay Plastik Inc. for injection molding.

Additional information

Some data in this study presented at IMSP'2010, Denizli-Türkiye were reported at the following thesis: O. Balkan, "The Effect of Thermoplastic Elastomers on the Mechanical Properties of Polypropylene Composites", Ph.D. Thesis, Marmara University, İstanbul, Türkiye, 2006.

References

[1] A.K. Gupta, S.N. Purwar, Crystallization of PP in PP/SEBS blends and its correlation with tensile properties, Journal of Applied Polymer Science 29/5 (1984) 1595-1609.
[2] A.K. Gupta, S.N. Purwar, Tensile yield behavior of PP/SEBS blends, Journal of Applied Polymer Science 29/5 (1984) 3513-3531.
[3] A.K. Gupta, S.N. Purwar, Studies on binary and ternary blends of polypropylene with SEBS, PS, and HDPE. I. Melt rheological behavior, Journal of Applied Polymer Science 30/5 (1985) 1777-1798.
[4] A.K. Gupta, S.N. Purwar, Studies on binary and ternary blends of polypropylene with SEBS, PS, and HDPE. II.

Tensile and impact properties, Journal of Applied Polymer Science 30/5 (1985) 1799-1814.
[5] A.K. Gupta, S.N. Purwar, Dynamic mechanical and impact properties of PP/SEBS blend, Journal of Applied Polymer Science 31/2 (1986) 535-551.
[6] S. Setz, F. Stricker, J. Kressler, T. Duschek, R. Mülhaupt, Morphology and mechanical properties of blends of isotactic or syndiotactic polypropylene with SEBS block copolymers, Journal of Applied Polymer Science 59/7 (1996) 1117-1128.
[7] F. Stricker, Y. Thomann, R. Mülhaupt, Influence of rubber particle size on mechanical properties of polypropylene-SEBS blends, Journal of Applied Polymer Science 68/12 (1998) 1891-1901.
[8] A. Bassani, L.A. Pessan, E. Hage, Toughening of polypropylene with styrene/ethylene-butylene/styrene tri-block copolymer: Effects of mixing condition and elastomer content, Journal of Applied Polymer Science 82/9 (2001) 2185-2193.
[9] F.O.M.S. Abreu, M.M.C. Forte, S.A. Liberman, SBS and SEBS block copolymers as impact modifiers for polypropylene compounds, Journal of Applied Polymer Science 95/2 (2005) 254-263.
[10] F. Ohashi, T. Hiroe, K. Fujiwara, H. Matsuo, Strain-rate and temperature effects on the deformation of polypropylene and its simulation under monotonic compression and bending, Polymer Engineering and Science 42/5 (2002) 1046-1055.
[11] R. Gensler, C.J.G. Plummer, C. Grein, H.-H. Kausch, Influence of the loading rate on the fracture resistance of isotactic polypropylene and impact modified isotactic polypropylene, Polymer 41/10 (2000) 3809-3819.
[12] H. Mae, Effects of local strain rate and micro-porous morphology on tensile mechanical properties in PP/EPR blend syntactic foams, Material Science and Engineering A 496 (2008) 455-463.
[13] A. van der Wal, R.J. Gaymans, Polypropylene-rubber blends: 3. The effect of the test speed on the fracture behaviour Polymer 40/22 (1999) 6045-6055.
[14] W. Jiang, S.C. Tjong, R.K.Y. Li, Brittle-tough transition in PP/EPDM blends: effects of interparticle distance and tensile deformation speed, Polymer 41/9 (2000) 3479-3482.
[15] H.H. Le, Th Lüpke, T. Pham, H.-J. Radusch, Time dependent deformation behavior of thermoplastic elastomers, Polymer 44/16 (2000) 4589-4597.
[16] C.D. Han, Multiphase flow in polymer processing, Academic Press, London, 1981.
[17] H. Eyring, Viscosity, plasticity, and diffusion as examples of absolute reaction rates, Journal of Chemical Physics 4/4 (1936) 283-291.
[18] K.A. Brown, R. Brooks, N.A. Warrior, The static and high strain rate behaviour of a commingled E-glass /Polypropylene woven fabric composite, Composite Science and Technology 70 (2010) 272-283.
[19] J. Ingram, Y. Zhou, S. Jeelani, T. Lacy, M.F. Horstemeyer, Effect of strain rate on tensile behavior of polypropylene and carbon nanofiber filled polypropylene, Material Science and Engineering A 489 (2008) 99-106.
[20] G.C. McGrath, Fracture and toughening in fibre reinforced polymer composites, in: rubber toughened engineering plastics, Chapman & Hall, 1994, 61.
[21] C.B. Bucknall, Toughened plastics, Applied Science Publishers Ltd, England, 1977.
[22] J. Wu, D. Yu, C.-M. Chan, J. Kim, Y.-W. Mai, Effect of fiber pretreatment condition on the interfacial strength and mechanical properties of wood fiber/PP composites, Journal of Applied Polymer Science 76/7 (2000) 1000-1010.
[23] S.C. Tjong, S.-A. Xu, Y.-W. Mai, Impact-specific essential work of fracture of maleic anhydride-compatibilized polypropylene/elastomer blends and their composites, Journal of Polymer Science B 40/17 (2002) 1881-1892.
[24] W.Y. Tam, T.Y. Cheung, R.K.Y. Li, Impact properties of glass fibre/impact modifier/polypropylene hybrid composites, Journal of Materials Science 35/6 (2000) 1525-1533.